PHYSICAL REVIEW B VOLUME 51, NUMBER 19 15 MAY 1995-I

Ensuring the constancy of the chemical potential within the local-density approximation for exchange and correlation: Implications for near-edge x-ray-absorption fine structure

V. L. Shneerson and W. T. Tysoe
Department of Chemistry and Laboratory for Surface Studies, University of Wisconsin–Milwaukee, P.O. Box 413, Milwaukee, Wisconsin 53201

D. K. Saldin
Department of Physics and Laboratory for Surface Studies, University of Wisconsin–Milwaukee, P.O. Box 413, Milwaukee, Wisconsin 53201

(Received 23 August 1994; revised manuscript received 20 January 1995)

We investigate the correct implementation of the exchange-correlation potential for the excited core electron in near-edge x-ray-absorption fine structure (NEXAFS). We examine the effects on NEXAFS spectra of the ground-state Slater and excited-state Dirac-Hara exchange potentials and current implementations of the Hedin-Lundqvist exchange-correlation potential on the muffin-tin model. For a test case of gas-phase acetylene, we find good agreement with prior experimental spectra only with the Hedin-Lundqvist potential implemented on the local-density approximation with a Thomas-Fermi-like requirement of constancy of the chemical potential.

I. INTRODUCTION

The phenomenon of x-ray-absorption near-edge structure (NEXAFS) refers to the strong modulations of the x-ray-absorption coefficient as a function of x-ray energy above the threshold for the excitation of an atomic core electron. NEXAFS covers the energy range up to about 50 eV above the edge. Beyond this range (up to 1 keV) only small oscillations of the absorption coefficient, known as extended x-ray-absorption fine structure (EXAFS), may be observed. Both EXAFS and NEXAFS originate from the modification of the photoelectron final state by the backscattering of the ejected photoelectron. Only the degree of the multiple scattering of the photoelectron is different.

For electrons ejected from the atomic cores with a relatively high energy, atomic-scattering factors exhibit a strong maximum in the forward-scattering direction. As a result, the x-ray-absorption coefficient is dominated by single-scattering processes. Although this simplifies the interpretation of EXAFS, the structural information which could be extracted from such spectra is limited to the atomic radial distribution function. In the NEXAFS region of the absorption spectrum, the ejected core electron explores its local environment through many multiple-scattering paths. This is the reason that NEXAFS gives much more structural information, e.g., the coordination geometry and the density and symmetry of the unoccupied valence electron states.

The second significant difference between NEXAFS and EXAFS is the role of exchange and correlation effects. The total energy E of an electron in a sea of other electrons may be written

$$E = K + V_H + V_{xc} , \tag{1}$$

where K is its kinetic energy; V_H its Hartree potential energy, which may be determined from the solution of Poisson's equation for the charge density of its environment; and V_{xc} is its exchange-correlation energy. It has become customary to treat V_{xc} as an extra contribution to the total potential energy of the electron. Also, the quantities V_H and V_{xc} are often loosely referred to as potentials (as we do in this paper) even though dimensionally they are energies.[1] A complication with the exchange-correlation potential V_{xc} is that, unlike V_H, it is a function of the kinetic energy K of the electron.

For an EXAFS photoelectron, only the high-energy asymptotic behavior of V_{xc} is of relevance. At such energies, as a rule, the exchange-correlation energy varies only slightly with K. Nevertheless, Mustre de Leon, Rehr, and Zabinsky[2] suggested that, even in EXAFS, use of an energy-dependent exchange-correlation potential for the excited final state is necessary for the best quantitative agreement with experiment. A NEXAFS photoelectron is even more sensitive to the energy dependence of the exchange-correlation interaction. The main purpose of this paper is to underline this sensitivity and to highlight ways of correct implementation of such an interaction in the theory of NEXAFS. We illustrate our points by considering C K-shell NEXAFS of a small gas-phase hydrocarbon molecule, acetylene.

The outline of the remainder of this paper is follows. In Sec. II we discuss the importance of the energy-dependent exchange-correlation potential for excited states in more detail, and compare the different known forms of that quantity. In Sec. III we make a critical study of the existing implementations of such potentials in NEXAFS calculations, and propose our own approach to the problem. In Sec. IV we present the results of our computer simulations of NEXAFS spectra for a gas-phase acetylene molecule to demonstrate the advantage of our proposed approach. Section V contains a summary and conclusions.

0163-1829/95/51(19)/13015(8)/$06.00

II. THE EXCHANGE-CORRELATION INTERACTION OF A NEXAFS ELECTRON

A NEXAFS photoelectron is created when an atomic core electron makes a transition to an unoccupied state above the Fermi level as a result of the absorption of an x-ray photon. The photoelectron radiates from the absorbing atom and experiences the electrostatic ion-core potential and the exchange-correlation potential of its environment. The exchange part of the latter potential arises from the anticorrelation between electrons of like spin due to the Pauli exclusion principle, while the correlation part may be thought of, roughly, as due to the Coulomb repulsion between all electrons. Since both these contributions lead to an anticorrelation among the electrons, they both cause a lowering of the mutual Coulomb interaction energy of the electrons, thus lowering the apparent potential energy of the photoelectron.

An x-ray-absorption spectrum is a plot of the absorption coefficient W as a function of the energy ω of the x-ray photon, where

$$\omega = E - E_c \ , \tag{2}$$

with E_c the energy of the core electron, the total energy E is specified by (1), and we take Planck's constant equal to unity. Combining (2) and (1) we note that

$$\omega = K + V_H + V_{xc} - E_c \ . \tag{3}$$

NEXAFS peaks correspond to constructive interference conditions in the multiple scattering of an ejected core electron within the neighborhood of the x-ray-absorbing atom. These are determined by the wavelength (or kinetic energy K) of that ejected electron. However, in general, the exchange-correlation energy V_{xc} is more negative for lower values of K (and hence x-ray frequency) than for higher values. Thus lower-energy NEXAFS peaks would be expected to be downshifted more than those of higher energy by the exchange-correlation energy. Consequently, an energy-dependent exchange-correlation energy would tend to increase the spacing between peaks on a NEXAFS spectrum. The results of Sec. IV will bear out this conclusion.

An early calculation of the exchange part V_{ex} of the potential energy of an electron in a uniform electron gas was made by Dirac,[3] and applied to electron spectroscopy by Hara.[4] The Dirac-Hara exchange potential is calculated using the Hartree-Fock approximation to a many-electron state, and assuming that the positive charges of the atomic nuclei are distributed uniformly (the jellium model). In Hartree atomic units, the Dirac-Hara exchange energy of an electron of kinetic energy K may be written

$$V_{DH}(x) = -\frac{(2E_F)^{1/2}}{\pi}\left[1+\frac{1-x^2}{x}\ln\left|\frac{1+x}{1-x}\right|\right] , \tag{4}$$

where E_F is the Fermi energy of the electron gas, and $x=(K/E_F)^{1/2}$. The potential energy V_{DH} is negative, and increases monotonically with x (and hence K), approaching zero asymptotically at high energies.

The Dirac-Hara potential (4) arises from the difference between the solutions of the Schrödinger equation for a free-electron gas in the Hartree and Hartree-Fock approximations.[5] So-called correlation effects arise if interactions between electrons of opposite spin are included. This can be done if the Schrödinger equation is replaced by the Dyson equation for the electron Green function $G(E,k)$,[6] where

$$G^{-1}(E,k) = E - K - \Sigma(E,k) \ . \tag{5}$$

In the above expression, k is the wave number of the electron, $K=k^2/2$ (in hartree) is its kinetic energy, E is the energy of an electron in an interacting electron gas, and $\Sigma(E,k)$ is the self-energy. The prescription for summing the significant Feynman diagrams which contribute to Σ is well known from quantum-field theory. Neglecting the vertex corrections to the electron-electron interaction, the self-energy (i.e., the exchange-correlation energy) of an electron excited above the Fermi level of a free-electron gas may be found from the integral

$$\Sigma(E,k) = i\int \frac{d^3q\, d\omega}{(2\pi)^4}\frac{V_H(q)}{\varepsilon(q,\omega)}G(E-\omega,k-q) \ , \tag{6}$$

where the Fourier coefficient $V_H(q)$ of the Coulomb potential is screened by the dielectric function $\varepsilon(q,\omega)$.

Hedin and Lundqvist have introduced the so-called GW approximation[6] for evaluating the integral (6), in which the function G on the right hand side is approximated by the Green function of a free electron. The resulting approximation to Σ is known as the Hedin-Lundqvist potential V_{HL}, which is characterized by its energy dependence, and its possession of an imaginary part, caused by inelastic processes such as the creation of electron-hole pairs and of plasmons. Other forms of the exchange-correlation potential, based on free-electron models, have also been proposed by other authors.[7–10]

A common feature of current practical electronic-structure calculations is the use of the local-density approximation (LDA).[11,12] This postulates that the exchange-correlation potential V_{xc} of an electron at a point $\mathbf{r}$ of density $n(\mathbf{r})$ in a nonuniform electron gas may be approximated by that of an electron in a uniform electron gas of the same local density. Using this approximation, the chemical potential μ may be derived by applying the variational principle to the total energy of the electron gas. As a result, μ may be considered a functional of the ground-state potential and of the kinetic energy of the electron gas. In x-ray absorption μ plays a crucial role since it determines the photon energy at the absorption edge. Therefore, as in the EXAFS theory of Lee and Beni,[13] we suggest that any approximate treatment of exchange and correlation should ensure that μ is constant throughout the material. We return to this point in Sec. III.

So far we have discussed the excited-state exchange-correlation energy. The relation of such a potential to the corresponding ground-state exchange-correlation energy employed in, for example, density-functional theory,[11,12] is conveniently illustrated by returning to the Dirac-Hara exchange energy (4). If this were integrated over all the occupied states, the resulting mean exchange

energy per electron (in hartree) is given[5] by the expression

$$V_{ex}=-(3/4\pi)(3\pi^2 n^{1/3}) , \quad (7)$$

where n is the density of the electrons. This dependence ($V_{ex}\propto n^{1/3}$) is common to all models of energy-independent ground-state exchange potentials, e.g., that from Slater's $X\alpha$ prescription.[14] In Sec. III we will also examine how to ensure the continuity of the exchange-correlation energy of an electron, excited from the atomic ground state to low-lying excited states.

III. CALCULATION OF THE EXCHANGE-CORRELATION POTENTIAL ON THE MUFFIN-TIN MODEL

A. Theory

Unlike the case of an isolated atom, the potential experienced by an electron in a sample of condensed matter has a very complicated spatial variation. A common representation of that potential that has proved to be very successful in the calculation of the electronic structure of metals,[15] which is in common use in the theoretical modeling of electron spectroscopies such as low-energy electron diffraction (LEED),[16] photoemission,[17] and x-ray absorption,[18] is the muffin-tin model. In this model, the potential in the vicinity of the atomic nuclei is taken to be of spherical symmetry up to a distance known as the muffin-tin radius, while the potential outside this radius, the interstitial potential, is taken as constant, equal to some average of the true potential that region.

One of the key problems in the calculation of x-ray-absorption spectra in this model is the determination of the threshold for photon absorption. This threshold has been identified by Mustre de Leon, Rohr, and Zabinsky[2] with the chemical potential μ of the interstitial regions between the muffin-tin spheres representing the atoms, where

$$\mu=k_F^2(\langle n_{int}\rangle)/2+V_{gr}(\langle n_{int}\rangle) , \quad (8)$$

with μ representing the local Fermi momentum, V_{gr} the ground-state interstitial potential energy (with respect to the vacuum level), and n_{int} the interstitial electron density. Note that, according to this prescription, both k_F and V_{gr} are approximated by their values for a uniform electron gas of the mean interstitial electron density $\langle n_{int}\rangle$. It has been claimed[2] that this approximation introduces tolerable errors of a few eV in the estimated chemical potential compared with self-consistent electronic structure calculations.

If an electron were excited to some energy E above the chemical potential in the interstitial region, its total potential energy may be written

$$V_{int}=V_{gr}+\delta V_{xc}(E,n_{int}) , \quad (9)$$

where $\delta V_{xc}(E,n_{int})$ is the energy-dependent part of the exchange-correlation energy above the Fermi level [taking $\delta V_{xc}(0,n_{int})=0$, and assuming that E is measured with respect to the chemical potential]. Thus the kinetic energy of an excited electron of total energy E in the interstitial region, where the potential is spatially invariant, is determined by the equation

$$k(E)^2/2=k_F^2(n_{int})/2+E-\delta V_{int}(E,n_{int}) , \quad (10)$$

where $k(E)$ is the energy-dependent wave number in the interstitial region, and the total electron energy E is measured with respect to the chemical potential μ, which in turn is determined by the ground-state exchange-correlation energy via Eq. (8).

Within a muffin-tin sphere, of course, the potential is a strongly varying function of position. However, a straightforward generalization of (9) within the spirit of the LDA enables the kinetic energy of a NEXAFS electron at a point $\mathbf{r}$, of local density $n(\mathbf{r})$ within a muffin-tin sphere, to be defined as

$$k^2(E,\mathbf{r})/2=k_F^2(n(\mathbf{r}))/2+E-\delta V_{MT}(E,n(\mathbf{r})) , \quad (11)$$

where $k(E,\mathbf{r})$ is an energy and position-dependent wave number within the muffin-tin sphere, $\delta V_{MT}(E,n(\mathbf{r}))$ is energy-dependent part of the exchange-correlation energy, and the local Fermi wave number is taken as

$$k_F(n(\mathbf{r}))=(3\pi^2)^{1/3}n^{1/3}(\mathbf{r}) . \quad (12)$$

A similar natural generalization of Eq. (8) also within the spirit of the LDA estimates the chemical potential within a muffin-tin sphere to be

$$\mu(\mathbf{r})=k_F^2(n(\mathbf{r}))/2+V_{MT}(n(\mathbf{r})) . \quad (13)$$

By definition, a chemical potential should be constant throughout a system. Indeed, if the energies E appearing in Eqs. (9), (10), and (11) are to refer to the same quantity, they must be measured from the same chemical potential. However, as we demonstrate below, the values of the chemical potential calculated from (8) and (13) are generally not in agreement.

To illustrate this point we consider a simple muffin-tin model of an artificial crystal of repeating units of the acetylene (C_2H_2) molecule. In order to approximate the potential of the gas-phase acetylene molecule as closely as possible, within the parameters of the muffin-tin model, the size of the unit cells containing each molecular unit was increased until no discernible changes in calculated x-ray-absorption spectra were observed.

Curve *a* of Fig. 1 depicts the variation of $\mu(\mathbf{r})$, as calculated from (13), within a C muffin-tin sphere of our artificial acetylene crystal. This chemical potential becomes more and more negative as the position of the atomic nucleus is approached since $V_{MT}(\mu,n(\mathbf{r}))$ becomes more negative deep within the atom faster than the Fermi energy $k_F^2(n(\mathbf{r}))/2\propto n^{2/3}(\mathbf{r})$ increases. The straight line b of Fig. 1 represents the estimate of the chemical potential in the interstitial region, as calculated by Eq. (8), It is obvious that prescriptions (8) and (13) above do not ensure the important physical requirement of the constancy of the chemical potential.

In order to overcome this problem in the application of the LDA, at least in non-self-consistent calculations, we borrow an idea from the Thomas-Fermi model: put the chemical potential first. The LDA may be used to calcu-

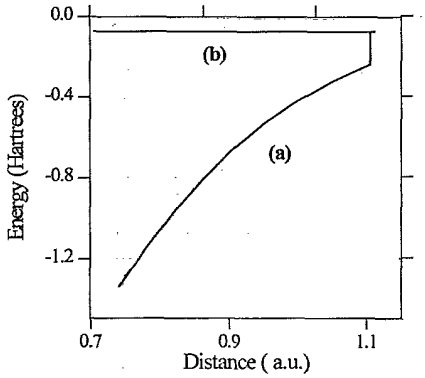

FIG. 1. Radial variation of the chemical potential μ within the C muffin tin of our model of an acetylene (C_2H_2) molecule. Line a: that calculated from Eq. (13), with both potential and kinetic energies estimated by LDA formulas. A discontinuity occurs at the muffin-tin radius of ~ 1.1 a.u., beyond which μ takes the value indicated by line b, the corresponding estimate for the interstitial region.

late the total potential $V_{\rm MT}$ within a muffin tin, but, in order to ensure constancy of the chemical potential, we suggest that the Fermi wave number within a muffin-tin sphere be evaluated not from (12) but from

$$k_F(\mathbf{r})=\{2[\mu-V_{\rm MT}(\mathbf{r})]\}^{1/2}\ , \tag{14}$$

with the chemical potential μ taken to be its value in the interstitial region, as calculated from (8). Equation (14) is essentially a law of energy conservation for an electron at the Fermi level throughout the material. Unlike definition (12), Eq. (14) enables k_F to "know" about not just the local electron density at the given point $\mathbf{r}$, but also about the electron distribution in the interstitial region, through the value of μ. To ensure consistency with the idea of a constant chemical potential, the wave number of an excited electron should be calculated not by (11), but by[12]

$$k(E,\mathbf{r})=\{2[E+\mu-V_{\rm MT}(\mathbf{r})-\delta V_{\rm MT}(E,k_F(\mathbf{r}))]\}^{1/2}\ . \tag{15}$$

It is worth noting that Eq. (15), introducing a local kinetic energy of the electron, is semiclassical by its nature (otherwise the kinetic energy at a given point does not exist). Of course, rather deep inside the muffin tin (atom), where the potential $V_{\rm MT}$ and the density n vary very rapidly, Eq. (15) is not valid. Fortunately, exchange and correlation potential in that region is negligibly small compared to $V_{\rm MT}$. Since we are concerned about the correct implementation of the exchange-correlation energy, only a thin spherical layer in the vicinity of the muffin-tin boundary is important. Within this layer, $V_{\rm MT}$ and n are smooth, slowly varying functions on the scale of $(k_F)^{-1}$ which satisfy the semiclassical requirements.

B. Determination of the muffin-tin zero

An important quantity within the muffin-tin model is the value assigned to the constant interstitial potential, $V_{\rm int}$, between the muffin-tin spheres, also known as the muffin-tin zero. Due to the energy dependence of the exchange-correlation potential, this quantity will also be energy dependent. In this subsection we compare different prescriptions for the calculation of this quantity.

The customary approach is to determine $V_{\rm int}$ as an average of the potential outside the muffin-tin spheres. Equation (9) indicates that this is a sum of ground-state and energy-dependent excited-state parts. In the work of Mustre, Rehr, and Zabinsky,[2] both these quantities have been calculated through the mean value $\langle n_{\rm int}\rangle$ of the interstitial charge density. Instead, we suggest that it is more appropriate to calculate the mean value of a function by averaging the function itself, not its argument. Simple statistical analysis confirmed that substantial differences follow from the different methods of averaging. For a grid of about 37 000 evenly spaced interstitial points for an acetylene (C_2H_2) molecule, we found that $\langle n_{\rm int}\rangle=0.063$ and $\langle n_{\rm int}^{2/3}\rangle=0.097$. Thus for, e.g., the Fermi energy E_F, which is proportional to $n^{2/3}$, quite different results are found depending on whether it is calculated via $\langle n_{\rm int}\rangle$ or $\langle E_F\rangle$, respectively. The fractional difference is $(\langle n_{\rm int}\rangle^{2/3}-\langle n_{\rm int}^{2/3}\rangle)/\langle n_{\rm int}^{2/3}\rangle$, i.e., about 60%.

Table I below compares the estimates of the energies (in hartree) of the ground-state Slater $X\alpha$ exchange energy V_S; the total interstitial potential energy $V_{\rm int}$, as estimated as the sum of V_S and the Hartree energy V_H; the Fermi energy $E_F(=k_F^2/2)$; and the chemical potential μ, as calculated by these two methods. The second column gives the value of the general quantity f, representing that in the first column, as determined by its value at the mean interstitial density $f(\langle n_{\rm int}\rangle)$. The third column gives the values of $(\langle f\rangle)$ found by averaging the quantities themselves. The percentage relative differences between the values in columns 2 and 3 are shown in the third column.

Similar differences are found in the values of the energy-dependent muffin-tin zero $V_{\rm int}(E,n_{\rm int})$ of the excited states. Figure 2 shows the results of calculating this quantity by four different algorithms: curve a depicts the result of calculating $V_{\rm int}(E,n_{\rm int})$ by the energy-independent Slater $X\alpha$ prescription.[14] Curve b was calculated from the formula

$$V_{\rm int}(E,n_{\rm int})=V_S(\langle n_{\rm int}\rangle)+\{V_{\rm DH}(E,\langle n_{\rm int}\rangle)-V_{\rm DH}(0,\langle n_{\rm int}\rangle)\}\ , \tag{16}$$

TABLE I. Estimates of the energy (in hartree) of the ground-state Slater $X\alpha$ exchange energy V_S. See text for details.

Quantity	$f(\langle n_{\rm int}\rangle)$	$\langle f\rangle$	Difference
V_S	−0.220	−0.127	73%
$V_{\rm int}$	−0.249	−0.157	59%
E_F	0.140	0.085	65%
μ	−0.110	−0.072	53%

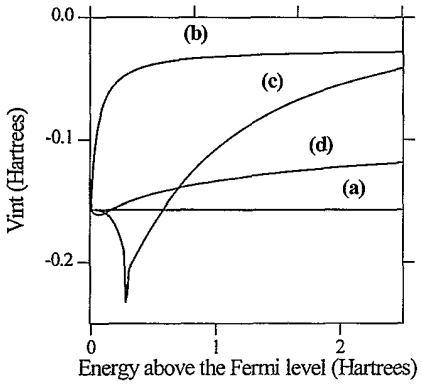

FIG. 2. Energy dependence of the muffin-tin zero $V_{\rm int}$ for the model acetylene molecule. The exchange-correlation potentials were calculated as follows. Line *a*: ground-state Slater $X\alpha$ exchange; lines *b* and *c*: Dirac-Hara exchange and Hedin-Lundqvist exchange-correlation, respectively, both evaluated at the mean interstitial electron density $\langle n_{\rm int}\rangle$. Line *d*: the result of averaging the Hedin-Lundqvist potential in the interstitial regions. All excited-state potentials were matched on to the ground-state Slater potential at the Fermi level.

in which the energy-dependent part of the potential is calculated by the Dirac-Hara expression (4), but is matched[2] on to the ground-state Slater exchange potential at the Fermi level, all potentials being evaluated for the mean interstitial density $\langle n_{\rm int}\rangle$. Curve *c* was calculated by the same expression except that the Hedin-Lundqvist potential $V_{\rm HL}$ replaced $V_{\rm DH}$ in (16). In our calculations $V_{\rm HL}$ was evaluated by the computer program developed by Mustre de Leon, Rehr, and Zabinsky[2] which is based on the additional plasmon-pole approximation of Lundqvist.[19] Finally, curve *d* was calculated from

$$\langle V_{\rm int}(E,n_{\rm int}(\mathbf{r}))\rangle=\langle V_S(n_{\rm int}(\mathbf{r}))+\{V_{\rm HL}(E,n_{\rm int}(\mathbf{r}))-V_{\rm HL}(0,n_{\rm int}(\mathbf{r}))\}\rangle\ , \tag{17}$$

which also employs the same Hedin-Lundqvist potential, but calculates the average of local LDA potentials, rather than that corresponding to the mean interstitial electron density $\langle n_{\rm int}\rangle$. Note that although curve *c* is characterized by a cusplike dip, due to the plasmon-pole approximation, this artificial feature completely disappears when the interstitial averaging is done by Eq. (17) rather than by one of the form (16). The reason is that the energy associated with the plasmon-pole cusp depends on the value of the density of the corresponding homogeneous electron gas. In our prescription (17), the interstitial potential is calculated from an average of Hedin-Lundqvist potentials, $V_{\rm HL}$, for a whole range of local densities $n_{\rm int}(\mathbf{r})$, rather than that for a single average density $\langle n_{\rm int}\rangle$. The resulting averaging of the cusps at different energies give rise to the smooth variation of the potential seen in curve *d*. We will see in Sec. IV that this contributes significantly to the improvement of the agreement between experimental and calculated NEXAFS spectra.

It should be noted that although expressions of the form of (16) and (17) ensure continuity of the exchange-correlation potential through the Fermi level, they give an incorrect asymptotic limit at high energies. The interstitial exchange-correlation energy (17), for instance, tends to a high-energy limit of $\langle V_S(n_{\rm int}(\mathbf{r}))-V_{\rm HL}(0,n_{\rm int}(\mathbf{r}))\}\rangle$, whereas strictly it should tend to zero. The justification for the use of expression (17) in our calculations below for NEXAFS spectra is that the excited-state electrons contributing to the spectra are much closer to the Fermi level than the high-energy limit. Thus one may argue that it is more important to ensure continuity of the exchange-correlation potential at the Fermi level than to strictly satisfy the correct high-energy limit.

C. The potentials within the muffin-tin spheres

In common with the approach of Ref. 2, we calculate both the kinetic and potential energies of an electron at the Fermi level in the interstitial region by some average of LDA prescriptions of those quantities (although our method of averaging differs from that of Ref. 2, as discussed above). This determines our chemical potential μ. Within a muffin-tin sphere the ground-state radial potential

$$V_{\rm MT}(r)=V_H(r)+V_{\rm xc}(n(r))\ , \tag{18}$$

where the exchange-correlation potential, $V_{\rm xc}$, is approximated by its LDA value, may be calculated by the usual Mattheiss prescription,[20] starting from, e.g., Herman-Skillman[21] self-consistent free-atom wave functions. Curve *a* of Fig. 3 represents the radial distribution of such a potential within a C muffin-tin sphere in our model of the acetylene molecule. A radial distribution of the local Fermi energy required to ensure that the total energy at the top of the Fermi sea is equal to μ may be calculated from Eq. (14).

To summarize, we propose that the muffin-tin zero be calculated from Eq. (17), the chemical potential by

$$\mu=\langle k_F^2(n_{\rm int}(\mathbf{r}))/2+V_{\rm gr}(n_{\rm int}(\mathbf{r}))\rangle\ , \tag{19}$$

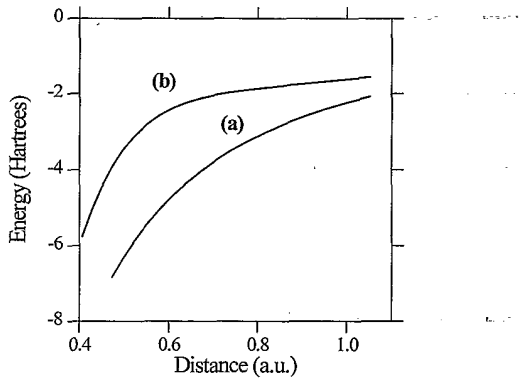

FIG. 3. Radial variation of the potential within a C muffin-tin sphere. Line *a*: calculated by the conventional LDA prescription, Eq. (18); line *b*: the fictional potential obtained by subtracting the LDA kinetic energy from the interstitial chemical potential.

and the local electron wave vectors from (14) and (15). We may term this prescription the constant chemical potential LDA or CCP-LDA.

It is interesting to note that, alternatively, one may choose to calculate k_F by the LDA formula (12) and evaluate a fictional ground-state potential by

$$V_{\rm fic}(\mathbf{r})=\mu-k_F^2(n(\mathbf{r}))/2 \ . \tag{20}$$

This potential is plotted as curve b of Fig. 3. A significant difference from the potential from the usual LDA Slater prescription for $V_{\rm MT}$ is observed. Thus it is clear that, in the usual LDA prescription (18), the potential within a muffin-tin sphere falls too fast toward the center of an atom to keep μ constant.

IV. COMPARISONS OF DIFFERENT PRESCRIPTIONS FOR THE EXCHANGE-CORRELATION POTENTIAL: NEXAFS FROM ACETYLENE

In this section we compare the effects of the different prescriptions for the calculation of the exchange-correlation potential for C K-shell NEXAFS from gas-phase acetylene C_2H_2. We compute the x-ray-absorption rate by the formula[18]

$$W(\omega)=W_{\rm at}(\omega)-2k\sum_{L,L'}M_{c,L}(E)\mathrm{Im}\langle L|\tau(E)|L'\rangle \times M^*_{c,L'}(E)\theta(E) \ , \tag{21}$$

where, in addition to the atomic transition rate $W_{\rm at}(\omega)$, there appears a modulation [the second term of (21)] due to multiple scattering by the surrounding atoms. The matrix elements of the photon-induced atomic transitions from a core state c to an excited state of energy E are denoted by $M_{c,L}$; the elements $\langle L|\tau|L'\rangle$ of the scattering path operator represent the effects of summing the multiple-scattering paths which begin and end on the central atom; the symbol $L[\equiv(lm)]$ represents the combination of angular momentum quantum numbers 1 and m, and $\theta(E)$ is a Heaviside function ensuring that the core electrons may be excited only above the Fermi level. By dividing the cluster into a set of concentric shells, a large number of atoms may be included in the calculations.[18] Multiple-scattering processes within each shell are included in turn. Due to inelastic damping, only those electrons which interact with a few nearby shells have a significant chance to be scattered back and affect the absorption rate. Practically, this means that only a few of shells are needed to achieve convergence. For our calculations we used an adaptation of the computer code of Vvedensky, Saldin, and Pendry.[22]

It is well known[22] that NEXAFS spectra are strongly dependent on the polarization of incident x rays. For the purposes of our discussion, we define a Cartesian coordinate system with its z axis defined by the direction of the C—C bond in the acetylene molecule. When the electric field e of the x rays is parallel to this direction, the resulting spectrum is dominated by a broad σ^* resonance from the overlap of the p_z orbitals from the two C atoms. When the electric field is perpendicular to that bond, a narrower π^* resonance peak appears, due to the overlap of the p_x and p_y orbitals. This is easy to understand, taking into account the polarization dependence of the absorption coefficient. For a z-polarized beam, only the $\langle 1,0|\tau|1,0\rangle$ element of the scattering path operator contributes.[22] Because of axial symmetry, the unoccupied σ^* orbital becomes more active as an absorbing mode with respect to the above-mentioned transition. A π^* resonance is more likely to be excited by x- and y-polarized x rays because of contributions of $\langle 1,\pm1|\tau|1,\pm1\rangle$ matrix elements.

Absorption of unpolarized x rays, however, would be expected to show up the presence of both the π^* and σ^* resonances on the same spectrum, since such a spectrum arises from an average overall direction of x-ray polarization. In the case of a gas-phase spectrum, of course, the multiplicity of molecular orientations results in such an average even for linearly polarized x rays. In Fig. 4 we show calculated NEXAFS spectra for C K-shell excitations from gas-phase acetylene. The three different spectra shown were calculated using existing prescriptions for the exchange-correlation potential. The first (curve a) was calculated assuming a ground-state Slater $X\alpha$ potential;[14] curve b employed the Dirac-Hara exchange potential (16), and curve c the corresponding Hedin-Lundqvist exchange-correlation potential, all following the LDA prescriptions of Mustre de Leon, Rehr, and Zabinski,[2] Since, probably, the absolute energies cannot be relied upon in these non-self-consistent calculations, the spectra were shifted in energy to align the π^* peaks on the three curves.

None of the calculated spectra of Fig. 4 give a good match to the experimental spectrum.[23] The ground-state $X\alpha$ potential (curve a) gives rise to a narrow π^* and a broad σ^* resonance, but their separation is more than 8 eV less than the experimental value. In the case of the LDA Hedin-Lundqvist potential (curve c), the interpeak separation is greater than the actual one by about 3 eV.

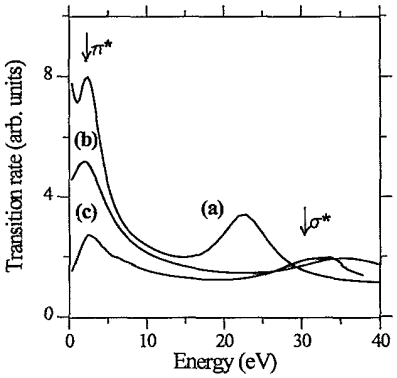

FIG. 4. Computer simulation of the C K-shell NEXAFS from gas-phase acetylene using different prescriptions for the exchange-correlation energy. Spectrum a: Assuming the ground-state Slater $X\alpha$ potential. Spectra b and c are from the Dirac-Hara and Hedin-Lundqvist potentials, respectively, implemented by the LDA scheme of Ref. 2. Experimentally measured positions of the π^* and σ^* resonances are indicated by arrows.

An even greater separation of the π^* and σ^* resonances is found for the Dirac-Hara potential (curve *b*).

Explanations for the different peak separations have already been discussed above. The variations of the energy-dependent muffin-tin-zero levels corresponding to each of the alphabetically numbered spectra of Fig. 4 are displayed as the corresponding numbered curves in Fig. 2. There is a correlation between the spacings of NEXAFS peaks and the energy variations of the muffin-tin zero. As pointed out above, the greatest spacing between the resonances occurs in the case of the Dirac-Hara potential for which the (negative) potential increases very rapidly with energy. On the other hand, the $X\alpha$ potential does not change with energy at all, and results in the smallest resonance spacing.

Curve *c* of Fig. 2 showed that if the muffin-tin zero were calculated assuming a Hedin-Lundqvist exchange-correlation potential for the mean interstitial electron density $\langle n_{\text{int}} \rangle$, it would reproduce the characteristic behavior of the artificial cusplike dip associated with the plasmon pole,[19] which in this case happens to be close to the π^*-resonance energy. This cusp affects the intensity of the corresponding NEXAFS peak. As the kinetic energy $(E - V_{\text{int}})$ increases, the electron backscattering amplitude becomes weaker, and so does the multiple-scattering resonance. Comparing spectra *c* of Figs. 4 and 5, which originate from the same muffin-tin potential with the muffin-tin zero values in Fig. 2 (curves *c* and *d*), it may be seen that the heights of the π^* peaks are inversely correlated with the kinetic energies of the electrons giving rise to them (the greater kinetic energies being associated with the deeper potentials).

Figure 5 shows the results of computer simulations for carbon *K*-edge NEXAFS of the gas-phase acetylene molecule C_2H_2, as calculated by our CCP-LDA scheme. The ground-state exchange was represented by the Slater $X\alpha$ potential V_S. Exchange-correlation effects of the excited states were included by our prescriptions (14), (15), and (17) for the implementation of the Hedin-Lundqvist potential V_{HL}. The relative positions, width, shape, and intensities of the two peaks are in good agreement with the experimental spectrum[23] (the experimental peak positions are indicated in Figs. 4 and 5 by arrows). The π^* resonance is narrow because it is more similar to its original ion-core state than the σ^* resonance to its constituent atomic states, due to the different degrees of overlap of the original atomic states.

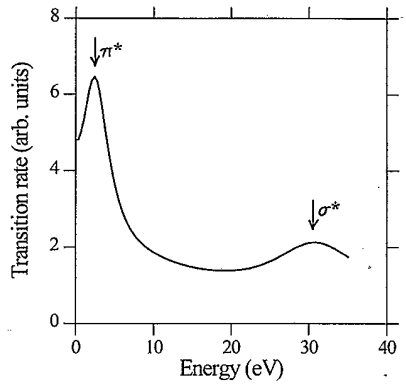

FIG. 5. Computer simulation of the C *K*-shell NEXAFS of gas-phase acetylene by the CCP-LDA method. Experimentally measured positions of the π^* and σ^* resonances are indicated by arrows.

V. CONCLUSIONS

It has been recognized that the energy-dependent exchange-correlation potential for a core electron excited by an x-ray photon can significantly affect the spacings of peaks on an EXAFS spectrum, and hence any structural conclusions drawn from Fourier transform techniques. The energy dependence of the exchange-correlation potential is even stronger for the lower-energy excited electrons contributing to a NEXAFS spectrum.

We have examined some common implementations of the exchange-correlation potential for EXAFS, such as the ground-state Slater and Dirac-Hara excited-state exchanges potentials and the Hedin-Lundqvist exchange-correlation potential, and examined their effectiveness in reproducing the NEXAFS spectrum of the gas-phase acetylene molecule. We find that, even in the case of the most sophisticated of these, namely the Hedin-Lundqvist potential, some prior approximations for its practical computation prevent it from correctly reproducing the experimentally observed separation of the π^* and the σ^* molecular resonances.

We make two suggestions for the correct implementation of the Hedin-Lundqvist potential on the muffin-tin model: first, that the ground-state interstitial potential be evaluated by averaging the potential in that region, and not by evaluating the interstitial potential at the average electron density; second, that both the Fermi energy and the kinetic energy of the excited NEXAFS electron be calculated from an algorithm that, like the Thomas-Fermi model, ensures that the chemical potential be constant throughout the material. We find that such an algorithm correctly reproduces the observed energy separation of the principal molecular resonances in acetylene.

ACKNOWLEDGMENTS

We are grateful to Professor John Rehr for his computer program for the calculation of the Hedin-Lundqvist exchange-correlation energy. V.L.S. acknowledges financial support from the Laboratory for Surface Studies of the University of Wisconsin–Milwaukee, W.T.T. support from the Department of Energy, Division of Chemical Sciences, Office of Basic Energy Sciences under Grant No. FG02-92ER14289, and D. K. S. a grant from the Petroleum Research Fund, administered by the American Chemical Society.

[1]D. K. Saldin and J. C. H. Spence, Ultramicroscopy **55**, 397 (1994).
[2]J. Mustre de Leon, J. J. Rehr, and S. I. Zabinsky, Phys. Rev. B **44**, 4166 (1991).
[3]P. A. M. Dirac, Proc. Cambridge Philos. Soc. **26**, 376 (1930).
[4]S. Hara, J. Phys. Soc. Jpn. **22**, 710 (1967).
[5]See, e.g., C. Kittel, *Quantum Theory of Solids* (Wiley, New York, 1987).
[6]L. Hedin and S. Lundqvist, in *Solid State Physics,* edited by H. Ehrenreich and D. Turnbull (Academic, New York, 1969), Vol. 23, p. 1.
[7]U. von Barth and L. Hedin, J. Phys. C **5**, 1629 (1972).
[8]O. Gunnarson and B. I. Lundqvist, Phys. Rev. B **13**, 4274 (1976).
[9]S. H. Vosko, L. Wilk, and M. Nusair, Can. J. Phys. **58**, 1200 (1980).
[10]J. P. Perdew and A. Zunger, Phys. Rev. B **23**, 5048 (1981).
[11]W. Kohn and L. J. Sham, Phys. Rev. **140**, A1133 (1965).
[12]*Theory of the Inhomogeneous Electron Gas,* edited by S. Lundqvist and N. H. March (Plenum, New York, 1983).
[13]P. A. Lee and G. Beni, Phys. Rev. B **15**, 2862 (1977).
[14]J. C. Slater, *The Calculation of Molecular Orbitals* (McGraw-Hill, New York, 1979), Vol. 5.
[15]V. L. Moruzzi, J. F. Janak, and A. R. Williams, *Calculated Electronic Properties of Metals* (Pergamon, New York, 1978).
[16]J. B. Pendry, *Low Energy Electron Diffraction* (Academic, London, 1974).
[17]J. B. Pendry, Surf. Sci. **57**, 679 (1976).
[18]P. J. Durham, J. B. Pendry, and C. H. Hodges, Comput. Phys. Commun. **25**, 193 (1982).
[19]B. I. Lundqvist, Phys. Konden. Mater. **6**, 206 (1977).
[20]L. F. Mattheiss, Phys. Rev. **133**, A1399 (1964).
[21]F. Herman and S. Skillman, *Atomic Structure Calculations* (Prentice-Hall, Englewood Cliffs, NJ, 1965).
[22]D. D. Vvedensky, D. K. Saldin, and J. B. Pendry, Comput. Phys. Commun. **40**, 421 (1986).
[23]A. Bianconi, *XANES Spectroscopy for Local Structures in Complex Systems,* Springer Series in Chemical Physics Vol. 27 (Springer-Verlag, Berlin, 1983), p. 118.